

Enhancement of Adhesion Properties, Corrosion Resistance and Cathodic Disbonding of Mild Steel-Epoxy Coating Systems By Vanadium Conversion Coating

M. S. Dehghan¹, M. M. Attar^{*2}

¹ Department of Mining and Metallurgical Engineering, Corrosion Group, Amirkabir University of Technology, P. O. Box: 15875-4413, Tehran, Iran

² Department of Polymer Engineering and Color Technology, Amirkabir University of Technology, P. O. Box: 15875-4413, Tehran, Iran

ARTICLE INFO

Article history:

Received: 31 May 2019

Final Revised: 07 Dec 2019

Accepted: 08 Dec 2019

Available online: 09 May 2020

Keywords:

Vanadium conversion treatment

Epoxy coating

Adhesion

Corrosion resistance

Cathodic disbondment

ABSTRACT

In this study, vanadium conversion coating (VCC) was deposited on the surface of soft-cast steel (St-37). A thermoset coating was enforced on the VCC and blank substrates. The surface was characterized by field emission scanning electron microscope (FE-SEM), elemental mapping of energy dispersive X-ray (EDX) and atomic force microscopy (AFM). The adhesion strength of the thermoset coating on the surface of the treated samples was measured before and after 35 days of submergence in 3.5 wt. % NaCl solution via a pull-off device. Meanwhile, the effect of VCC treatment on the thermoset coating (epoxy) was examined by electrochemical impedance spectroscopy (EIS) and cathodic delamination (CD) tests. FE-SEM, EDX and AFM studies of treated surfaces showed a homogeneous vanadium oxide/hydroxide layer precipitated on the metal which increased the surface roughness. It was shown that VCC significantly improved the corrosion resistance of the epoxy coating. The vanadium compounds also reduced the cathodic activity on steel resulting in lower cathodic disbandment. The lower adhesion loss was also observed on the vanadium treated sample in comparison with the blank one. Prog. Color Colorants Coat. 13 (2020), 223-238 © Institute for Color Science and Technology.

1. Introduction

Many kinds of organic coatings used to protect the steel substrate in a corrosive media are thermoset systems. Thermoset organic coatings can control the charge transport because of high cross-linking density, which increases the ionic resistance. Epoxy coatings are one of thermoset organic coatings which are extensively used in metal protection owing to their excellent adhesion, acid/alkali and solvent resistance, mechanical properties and cross-linking density [1]. However, most of them are permeable against oxygen, water and destructive ions, which is due to weakness sites, micro porosities and cavities inside the coating matrix produced during

coating utilization and curing processes [2-4]. The diffusion of destructive species into the coating/metal interface leads to the damaging of the coating, reducing the barrier characterization of the coating and annihilation of the adhesion bonds in different ways. Hydroxyl ions created in the cathodic area beneath the coating lead to the increase in pH, which weakens the coating adhesion and delaminates the coating due to the penetration of electrolyte beneath the coating [5-9]. The water molecules may place themselves at the coating/metal interface and thereby destruct adhesion bonding through producing hydrogen bonds with metal or hydrolysis of the oxide layer on the metal surface. An

*Corresponding author: attar@aut.ac.ir

effective approach to dominate these problems is applying chemical and electrochemical conversion treatments, which provide stronger and more stable adhesion bonds between the substrate and the coating. In this regard, various kinds of conversion coatings (CCs) have been exerted. Conversion coatings can increase the adhesion of epoxy coating to the metallic layers by increasing the energy level or changing the surface morphology [10-14]. Hexavalent chromates (Cr^{6+}) and phosphates were widely used as conventional applied conversion coatings on metal substrates. Nonetheless, phosphate-base treatment is being substituted by diverse alternatives because of sludge formation, long immersion times and high energy consumption [15-20]. In addition, the environmental issues of the chromium(VI) compound is a major challenge [21-27]. Hence, Cr(III) conversion coating was replaced with Cr (VI) with fewer toxic properties. However, it has been shown that Cr(III)-based conversion coatings cannot provide corrosion resistance and suitable adhesion of organic coating to the steel surface like Cr (VI) [24, 28-31]. Lower thickness of Cr(III) conversion coatings compared to Cr(VI) is responsible for the low corrosion resistance of this coating. To solve these problems, the environmentally acceptable different conversion coatings such as molybdenum [32-34], cerium [35-37], zirconium [12, 38], titanium [39, 40], Lanthanum [41] and vanadium [42-49] have been reported. Recently, some papers reported the application of vanadate conversion treatments on aluminum alloys and magnesium alloys as a replacement for Cr (VI)-based conversion coatings [45-49]. Hamdy et al. [22, 50, 51] identified that Vanadium conversion treatment has a special self-reforming potency similar to chromate conversion coatings for magnesium alloys, although its barrier protection is poor (the value of $|Z|$ is less than $1000 \Omega \text{ cm}^2$). Yang et al. [48] indicated that the vanadate conversion treatment has the ability to replace chromate conversion treatment. These results illustrated that the VCC on metal surfaces is composed of vanadium and oxygen forms such as V^{5+} and V^{4+} , e.g. V_2O_5 , VO_2 , and

their hydrates for example $\text{V}_2\text{O}_5 \cdot n\text{H}_2\text{O}$, $\text{VO}(\text{OH})_2$ and $\text{VO}(\text{OH})_3$ compounds [44, 47, 48]. Utilizing VCC on the surface of mild steel is a modern and effective procedure as a substitute for conventional surface treatments [52].

The objective of this manuscript is to study the effect of Vanadium conversion treatment (VCC) on surface morphology, corrosion properties, adherence and cathodic disbondment of epoxy coatings. Surface morphology was studied by FE-SEM and AFM analyses. Meanwhile, epoxy coatings applied on the steel surface with and without VCC and their properties were studied by EIS, pull-off adhesion and cathodic delamination tests.

2. Experimental

2.1. Materials

St-37 mild steel sheets ($10 \times 10 \times 0.2 \text{ cm}^3$) were supplied from Mobarake steel Co., Iran. The chemical composition of the steel sheets is given in Table 1. Treatment baths were prepared using hydrochloric acid (37 wt.%), sodium hydroxide and V_2O_5 , which were purchased from Merck Co.

EPON 828 Resin (Bisphenol-A diglycidyl ether epoxy resin) and polyamine hardener (Epikure F205) were purchased from Shell Co. (USA) and Kian Co. (Iran), respectively. Beeswax-colophony mixture (3:1.2) was also used to seal the coated specimens.

2.2. Surface preparation

Steel sheets were abraded by emery paper 800 followed by degreasing using acetone. Then, the cleaned steel sheets were immersed in 200 mL VCC bath containing $50 \text{ mg L}^{-1} \text{ V}_2\text{O}_5$. The VCC layer was applied on the steel substrate at room temperature. The pH of the VCC bath was adjusted at 3 and the vanadium treatment was carried out for 60s. Then, the VCC samples were washed with deionized (DI) water and dried immediately by warm air flow.

Table 1: Chemical composition of St-37 steel sheet.

| Elements | Fe | C | Si | Mn | P | S | Al |
|---------------------|-------|------|------|------|------|------|------|
| Composition (wt. %) | 99.03 | 0.18 | 0.33 | 0.32 | 0.05 | 0.05 | 0.04 |

2.3. Coating application

The epoxy coating formulation was prepared using Epon 828 resin based on Bisphenol-A diglycidyl ether epoxy resin (DGEBA) with Epoxide Equivalent Weight, Viscosity and density of 185-192, 110-150 and 1.17 g cm^{-3} at 25°C , respectively. 100 g of the EPON 828 resin was blended with 55 g Epikure F205 curing agents. The coatings were applied on the mild steel substrates with and without VCC by a film applicator (Elcometer 3520 Baker) and the coated samples kept under ambient condition (i.e. $24 \pm 2^\circ\text{C}$ and $30 \pm 3\%$ RH). Finally, Coatings (VCC+ epoxy and blank epoxy) were cured for 7 days. The dry thicknesses of whole coatings were about $40 \pm 5 \mu\text{m}$.

2.4. Methods

2.4.1. Surface examination

The surface morphology of mild steel treated with vanadium-based conversion coating was studied by Mira III-XMU(Czech Republic) field emission scanning electron microscope (FE-SEM) equipped with Energy Dispersive X-ray (EDX) detector with 8 keV accelerating voltage.

Surface topography was also studied on the samples in tapping mode by AFM (model Ara 1010/A, Iran) using a silicon cantilever with a frequency of 180 kHz and image scan rate of 2 Hz. Total average and mean square roughness parameters of the studied samples were estimated by image processing software (version 1.01).

2.4.2. Pull-off experiment

Epoxy coatings were applied on the mild steel substrates without and with VCC treatment. Pull-off testing of the coatings was implemented according to ASTM D-4541. Adhesion of epoxy coatings to the undercoat was determined by a Posi test pull off adhesion tester (DEFELSKO). The test was performed on the specimens before and after 35 days immersion in 3.5 wt.% sodium chloride solution. The aluminum test Pull-Stubs (dollies) of 14.2 mm diameter were connected to the surface of the epoxy coatings with Araldite 2017 adhesive. Samples were exposed to air for 48 h to ensure that the Araldite adhesive was entirely cured. Then, a gap was created around dollies and pulling was applied at 7 mm/min. The experiments were done on three replicates.

2.4.3. Electrochemical analysis

The effect of VCC on the corrosion resistance of epoxy coating was evaluated by an AUTOLAB Potentiostat-Galvanostat (PGSTAT302N). The tests were conducted at open circuit potential (OCP) on 1 cm^2 in 3.5 wt.% NaCl solution for 35 days. To perform electrochemical tests, we applied a three electrode system configuration consisting of the coated steel sample as working electrode (WE), platinum auxiliary electrode (AE) and a silver-silver chloride electrode (Ag/AgCl) (3 M KCl) as reference electrode (RE). The frequency range and amplitude of sinusoidal voltage were 10 kHz to 10 mHz (peak to zero) and 10 mV, respectively. The experiments were done on three replicates.

2.4.4. Cathodic disbondment test

The cathodic disbondment of the epoxy coatings applied on the untreated and VCC specimens was studied in a solution containing 1 wt.% each of sodium carbonate, sodium chloride and sodium sulfate at $\text{pH} = 12$ (ASTM G8). For this object, a dummy cavity of 1 mm in radius was created in the center of the samples by eliminating of the epoxy coatings from the metal surface (with exposed area of $3 \times 3 \text{ cm}$) and then they were immersed in the test solution under potential polarization of -1.5 V (versus Ag/AgCl reference electrode) for 15 h. After the polarization, the system was dismounted from the samples and the average disbonding area was measured.

3. Results and Discussion

3.1. Surface characterization of VCC samples

3.1.1. FE-SEM/EDX analysis

The surface morphology of the samples was investigated by FE-SEM technique before and after VCC treatment. The FE-SEM micrographs of the samples are shown in Figure 1. Figure 1a shows the surface of bare steel including meaningful lines that are caused due to the preparation of surface by grit paper. Significant changes are observed after the VCC treatment (Figure 1b). From Figure 1b, it can be observed that VCC layer is composed of nanoparticles close together. However, after formation of the VCC film on the metal surface (Figure 1c), a homogeneous, dense, uniform and thin layer containing small-sized particles is created on the steel surface. The appearance of the nanoparticles in the VCC film reflects its higher

nucleation rate compared to the growth rate of vanadium compounds, so very fine particles are deposited on the VCC layer. Also, there are some defects and porosities (nano and micro) in the sample (Figure 1c). These porosities may be due to the release of hydrogen from the chemical reaction during the coating process [22, 51]. Hence, corrosive electrolyte may easily penetrate into the VCC layer and a harsh corrosion occurs after an extremely long time immersion in corrosive environments.

The diameter of the nanoparticles deposited on the VCC layer was investigated by Image J software [53]. The diameter of the most of nanoparticles in the VCC layer is less than 30 nm (Figure 2b).

The EDX analysis of mild steel with and without VCC via elemental mapping of V, O and Fe-V is shown in Figure 3. Meanwhile, the results derived from these images are given in Table 2. Additional peak in 5 Kev is related to the sediment of vanadium compounds. Elemental analysis shows almost homogeneous distribution of oxygen and vanadium on the surface of the VCC. In addition, VCC film is not continuous according to the elemental mapping of Fe-V.

From Table 2, it can be considered that V, Mn, Fe and Si are the elements which were detected on the steel surface treated by VCC. Also, it can be understood that the amount of Fe significantly decreased after VCC formation. Detection of V on the samples with VCC indicates that a thinner vanadium compound film was formed on the surface of the sample.

The overall reaction to form VCC has been suggested as a result of the dissolution of the steel as an anodic reaction and hydrogen reduction as a cathodic reaction. Hydrogen reduction with the hydroxyl ion causes the evolution of cathodic sites which increases the local pH in the interface of the metal/vanadium solution. Vanadium bath includes V^{5+} ions in the acidic pH which turns to VO^{2+} . Jiang [42], Guan [47] and Zou [54] used electron spectroscopy for chemical analysis (ESCA) and proved that an increase in surface pH leads to the formation of V_2O_5 and $VO(OH)_3$. The proposed reactions are as follow equations 1 and 2:

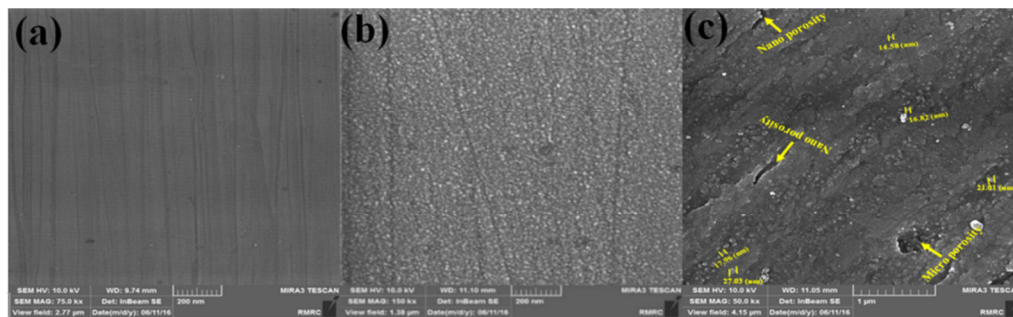
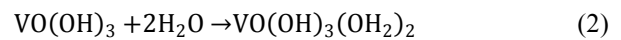
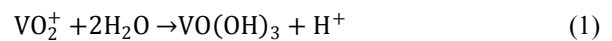


Figure 1: FE-SEM micrographs from the surface (a) blank sample and (b, c) VCC samples.

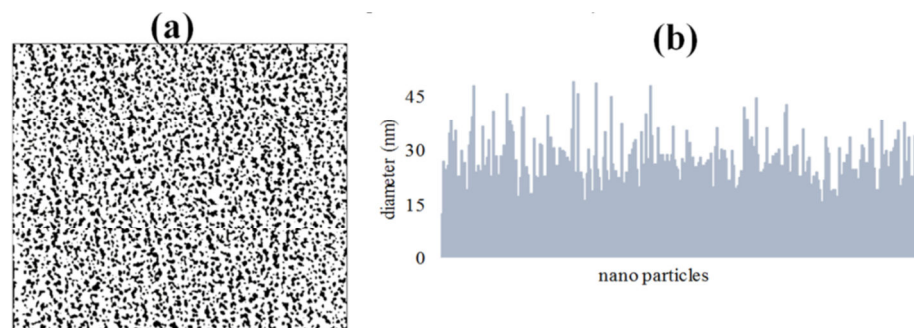


Figure 2: Nanoparticle size analysis using Image J software (a) threshold for an image with bright particles and (b) diagram of nanoparticles diameter.

Table 2: The elemental composition obtained by EDS map.

| Element | V | Fe | Si | Mn |
|---------------|------|-------|------|------|
| blank sample | - | 99.22 | 0.27 | 0.24 |
| VCT treatment | 0.39 | 96.85 | 0.28 | 0.26 |

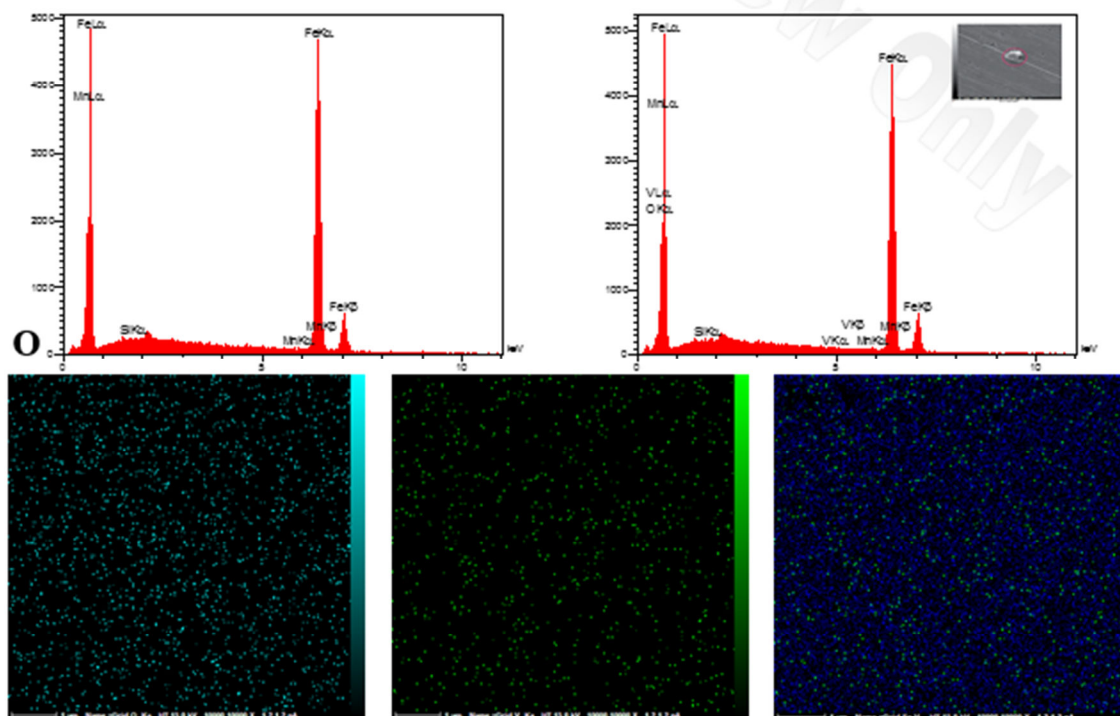


Figure 3: EDX diagrams from mild steel with and without VCC obtained by SEM-EDX elemental mapping of V, O and Fe-V.

3.1.2. AFM

AFM topography of the samples before and after immersion in VCC solution is shown in Figure 4. Topographic images are captured in AM-mode on a $5 \times 5 \mu\text{m}^2$ surface. Figure 4a shows that the surface pattern includes parallel lines owing to the surface preparation by mechanical polishing (sand paper). A comparison between two images shows that the scale of samples before and after immersion in vanadium conversion solution is in the range of nanometer. Results from Figure 4 show that the surface roughness of the sample increased after applying VCC. The surface roughness including R_a (Average roughness), R_t (total roughness) and R_{rms} (Root Mean Square roughness) were calculated according to the AFM three-dimensional images as well as equations 3, 4 and 5 [55] as shown in Table 3.

$$R_a(N,M) = \frac{1}{N} \sum_{x=1}^N (Z(x,y) - \bar{Z}(N,M)) \quad (3)$$

$$R_t = R_p - R_v \quad (4)$$

$$R_{rms}(N,M) = \sqrt{\frac{1}{N} \sum_{x=1}^N (Z(x,y) - \bar{Z}(N,M))^2} \quad (5)$$

which R_v and R_p are the maximum profile peak height and maximum profile valley depth, respectively. It is observed that roughness of the surface increased in the presence of VCC. It is reported that the bottom levels may play a notable role for the coating adhesion properties [56]. AFM examination demonstrates an improvement in the roughness of the mild steel surface up to about 80 nm when VCC treatment was used on the mild steel.

3.2. Pull-off measurements

Epoxy/polyamine coating was used on the surface of steels with and without VCC treatment. The adhesion of the samples was specified by pull-off techniques. The values of adhesion of the epoxy coated samples with and without surface treatments are presented in Figure 5 which shows that VCC treatment of steel caused an enhancement in pull-off strength of the epoxy coating over the steel substrate. VCC increased the adhesion strength through increasing the surface free energy and surface roughness. Observing a mixture of adhesive and cohesive failure for samples with VCC showed that VCC significantly increased the coating adhesion properties on the steel surface.

The adhesion properties of the samples were also investigated after 35 days immersion in 3.5 wt.% NaCl solution. The recovery adhesion strength (after 35 days immersion) values were evaluated. Afterwards, the adhesion loss was calculated according to equation 6.

$$\text{Adhesion loss(\%)} = \frac{\text{Dry adhesion strength} - \text{recovery adhesion strength}}{\text{Dry adhesion strength}} \times 100 \quad (6)$$

According to Figure 5, it can be assumed that the adhesion loss values of the epoxy coatings applied to the samples with VCC are less than that of untreated sample. The adhesion loss values for epoxy coating on VCC surface is 44% and it is 66% for untreated one. It is well accepted that the diffusion of water, oxygen and aggressive ions into the epoxy coating/steel interface is explanation for the coating adhesion loss. Hydroxyl ions (OH^-) are formed from cathodic reaction of equation 7 at the interface of epoxy coating/metal. This can cause an increase in pH beneath the coating and destroys adhesion bonds. Nonetheless, conversion coating reduced the adhesion loss through: 1) Formation of strong adhesion bonds between the organic coating and the steel substrates, 2) Blocking of the cathodic sites which inhibits the cathodic reactions on the steel substrate and 3) Reduction of cathodic and anodic reaction rates through preventing the corrosive agents from reaching to cathode and anode sites.



Table 3: Roughness values obtained from AFM analysis for the untreated and VCC treated.

| Sample | R_a (nm) | R_t (nm) | R_{rms} (nm) |
|-----------|------------|------------|----------------|
| Untreated | 1.838 | 21.98 | 18.65 |
| VCT | 6.551 | 69.33 | 66.48 |

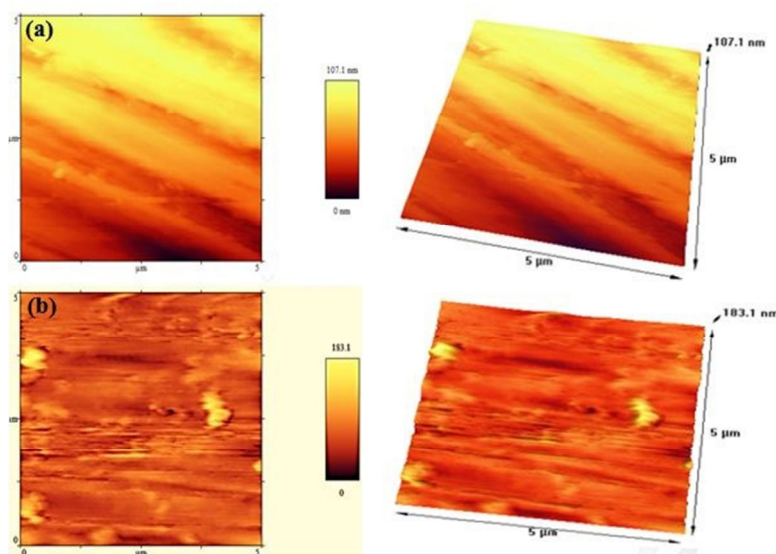


Figure 4: 2D and 3D AFM micrographs of (a) untreated and (b) VCC treated.

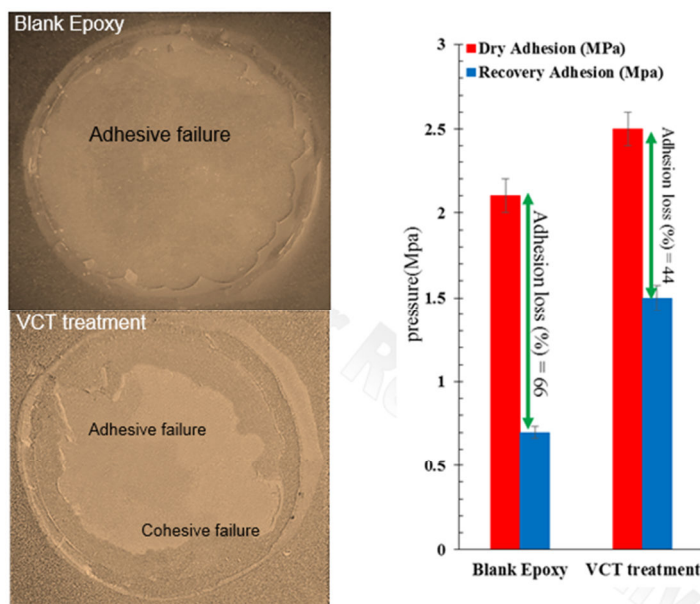


Figure 5: Dry and recovery adhesion strengths of Blank epoxy and VCC/epoxy samples after 35 days immersion in 3.5 wt.% NaCl solution, adhesion loss values and digital photos of tested samples after pull-off test.

The coating failure exposed to 3.5 wt.% NaCl may be attributed to the fact that diffusion of ions and water from the electrolyte to the metal/coating interface can significantly reduce the adhesion bonding between the metal surface and epoxy coating. The VCC layer consists of vanadium oxide/hydroxide compounds which can cause a strong electrostatic attraction between polar groups of epoxy coating and metal surface containing VCC. Moreover, the higher physical bonding strength in samples with VCC treatment is due to the increment of roughness, surface free energy and lower water contact angle [52].

3.3. EIS measurements

The impact of VCC at different reaction times on the corrosion and ionic resistances of the epoxy coating was studied by EIS technique. The EIS analysis was done after 3, 15 and 35 days immersion in 3.5 wt.% NaCl solution. The Nyquist and Bode graphs of various specimens after 35 days immersion are shown in Figures 7 and 8. The experimental results were fitted with electric equivalent circuit data and used for comparison. Suitable electrical circuits for samples with one-time constant and two-time constant are indicated in Figures 6, 7 and 9.

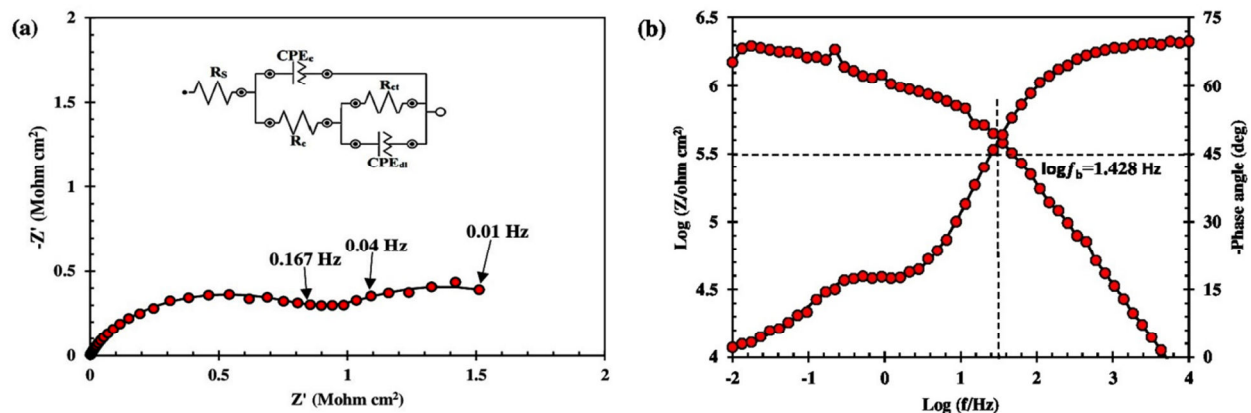
The experimental results were fitted including: R_p (polarization resistance), R_{ct} (charge transfer resistance), R_c (coating resistance), CPE_c (Constant phase element of coating) and CPE_{dl} (double-layer capacitance). Impedance factors are extracted from the model and displayed in Table 4. Figure 6 shows the Nyquist and Bode graphs of the blank epoxy samples. It can be obviously seen from the results that the oxygen, water and corrosive ions (Cl^-) permeate below the coating. The coating behavior at a vast frequency range is mostly resistive and the capacitive behaviors can be seen at very high frequencies. Hence, the corrosive electrolyte could penetrate into the coating matrix through micro porosities, channels, holes, free volumes and defects in the coating which were frequently created during processing. Nyquist and Bode plots of epoxy coatings applied to steel substrates without and with VCC are shown in Figures 7 and 8, respectively. The results show that the reduction in the corrosion resistance of samples treated with VCC is less than that of blank epoxy.

Examination of capacitive region and maximum phase angle at a wider frequency zone compared to the blank epoxy reveals the improvement of the barrier performance of the coating in the presence of VCC.

Table 4: The electrochemical parameters of the impedance plots of the blank epoxy, VCC/epoxy samples immersed in 3.5 wt.% NaCl solutions for 3, 15 and 35 days.

| Sample | $R_c^a (M\ ohm\ cm^2)$ | CPE_c | | $R_{ct}^d (M\ ohm\ cm^2)$ | CPE_{ct} | |
|----------------------|------------------------|-------------------------------------|-------|---------------------------|-----------------------------------|------|
| | | $Y_0^b (\Omega^{-1}\ cm^{-2}\ s^n)$ | n^c | | $Y_0 (\Omega^{-1}\ cm^{-2}\ s^n)$ | n |
| Blank epoxy (3days) | 4387 | 4.6×10^{-10} | 0.90 | - | - | - |
| Blank epoxy (15days) | 22 | 7.4×10^{-9} | 0.80 | 0.14 | 7.9×10^{-8} | 0.84 |
| Blank epoxy (35days) | 1.01 | 3.1×10^{-8} | 0.78 | 0.91 | 7.8×10^{-7} | 0.83 |
| VCT/epoxy (3days) | 7190 | 4.3×10^{-10} | 0.91 | - | - | - |
| VCT/epoxy (15days) | 47 | 6.1×10^{-9} | 0.79 | 38 | 6.1×10^{-8} | 0.87 |
| VCT/epoxy (35days) | 2.1 | 2.6×10^{-8} | 0.76 | 1.7 | 6.3×10^{-7} | 0.80 |

- a. The standard deviation range for R_c values is between 4% and 6.0%.
 b. The standard deviation range for Y_0 values is between 3.5% and 5.6%.
 c. The standard deviation range for n values is between 1% and 2%.
 d. The Standard deviation range for R_{ct} values is between 1.5% and 3.5%.

**Figure 6:** Impedance data obtained from EIS analysis for the sample immersed in 3.5 wt.% NaCl solution for 35 days, (a) Nyquist and (b) Bode plots.

The impedance values at 10 mHz (low frequency limit) and breakpoint frequency (f_b : frequency at 45° phase angle) for different samples are compared in Figure 9. The $|Z|_{10\text{ mHz}}$ shows the total resistance, including the solution resistance, charge transfer resistance and epoxy/VCC coating resistance. Hence, $|Z|_{10\text{ mHz}}$ indicates resistive behavior at low frequency region due to higher diffusion of corrosive agents. It can be seen from Table 4 and Figure 9a that the corrosion properties and electrical resistance values (impedance) at low frequency were reduced notably after 35 days immersion. Results showed that a decline in the corrosion resistance of the samples modified of VCC is lower than the blank surface. Therefore, surface modification of the steel surface by VCC treatment increased the corrosion resistance of the epoxy coating. This means that the VCC treatment has a notable impact on enhancing the corrosion resistance of epoxy coatings. In other words, the VCC treatment can limit the access

of the corrosive agents to the active sites on the steel surface.

The coating delamination and corrosion products can be studied by breakpoint frequency (f_b). The breakpoint frequency shows that the electrolyte diffusion into the coating/metal interface is responsible for the microscopic delamination of the coating. The enhancement of f_b shows the increase of delaminated area [57, 58]. Figure 10b shows the increase of f_b after 35 days of immersion. The lowest increase of f_b was observed for the modified sample by VCC.

The microscopic delaminated area of the coating on the VCC sample is lower than blank sample. All of these observations show that the VCC chemical treatments could enhance the corrosion protection properties of the epoxy coating through enhancing the adhesion properties. The VCC chemical treatments could inhibit the cathodic reactions through decreasing the electrochemical activity of the steel surface.

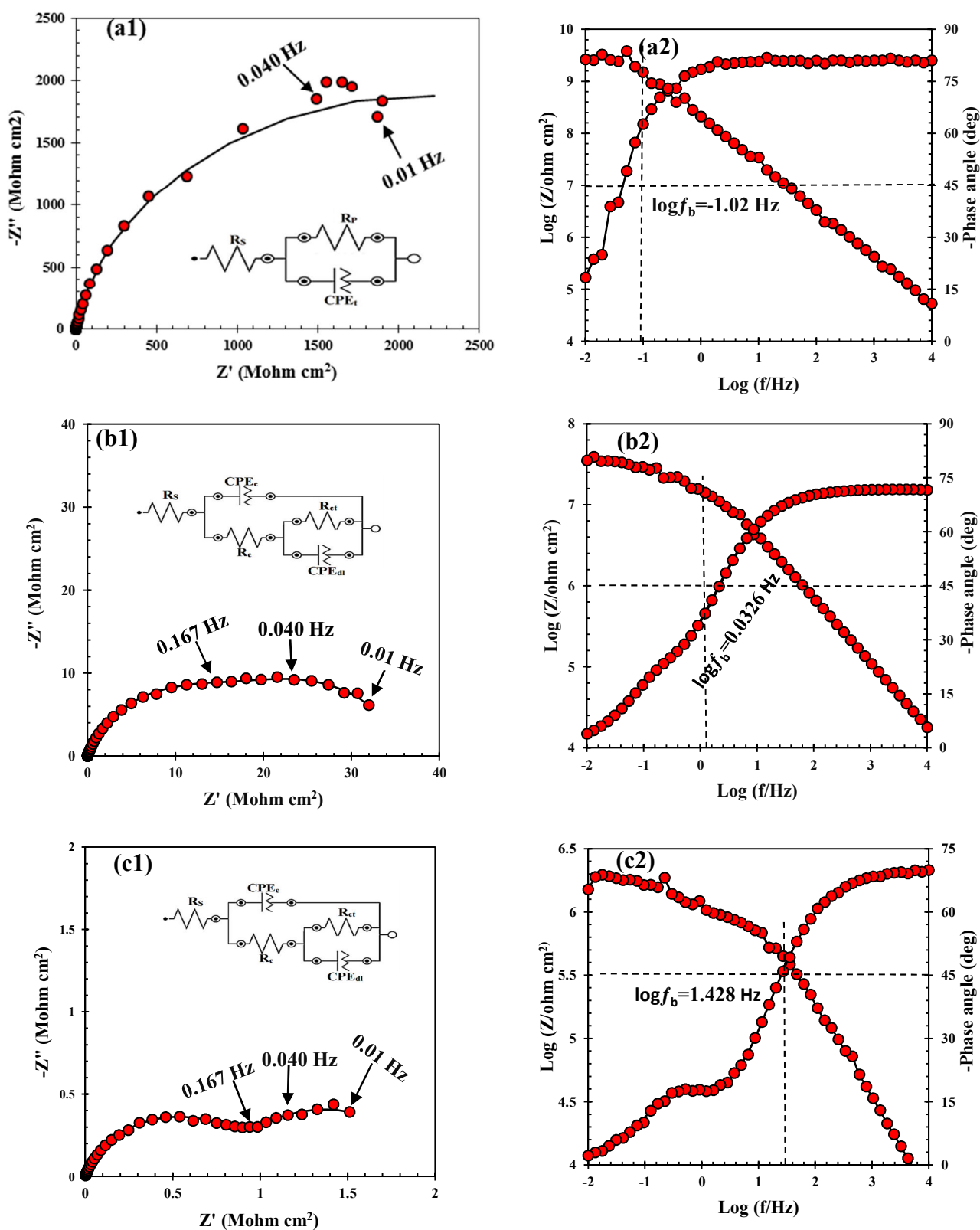


Figure 7: (a1, b1 and c1) Nyquist and (a2, b2 and c2) Bode plots of the blank epoxy coating subjected to 3.5 wt% NaCl solution for (a1, a2) 3, (b1, b2) 15 and (c1, c2) 35 days immersion.

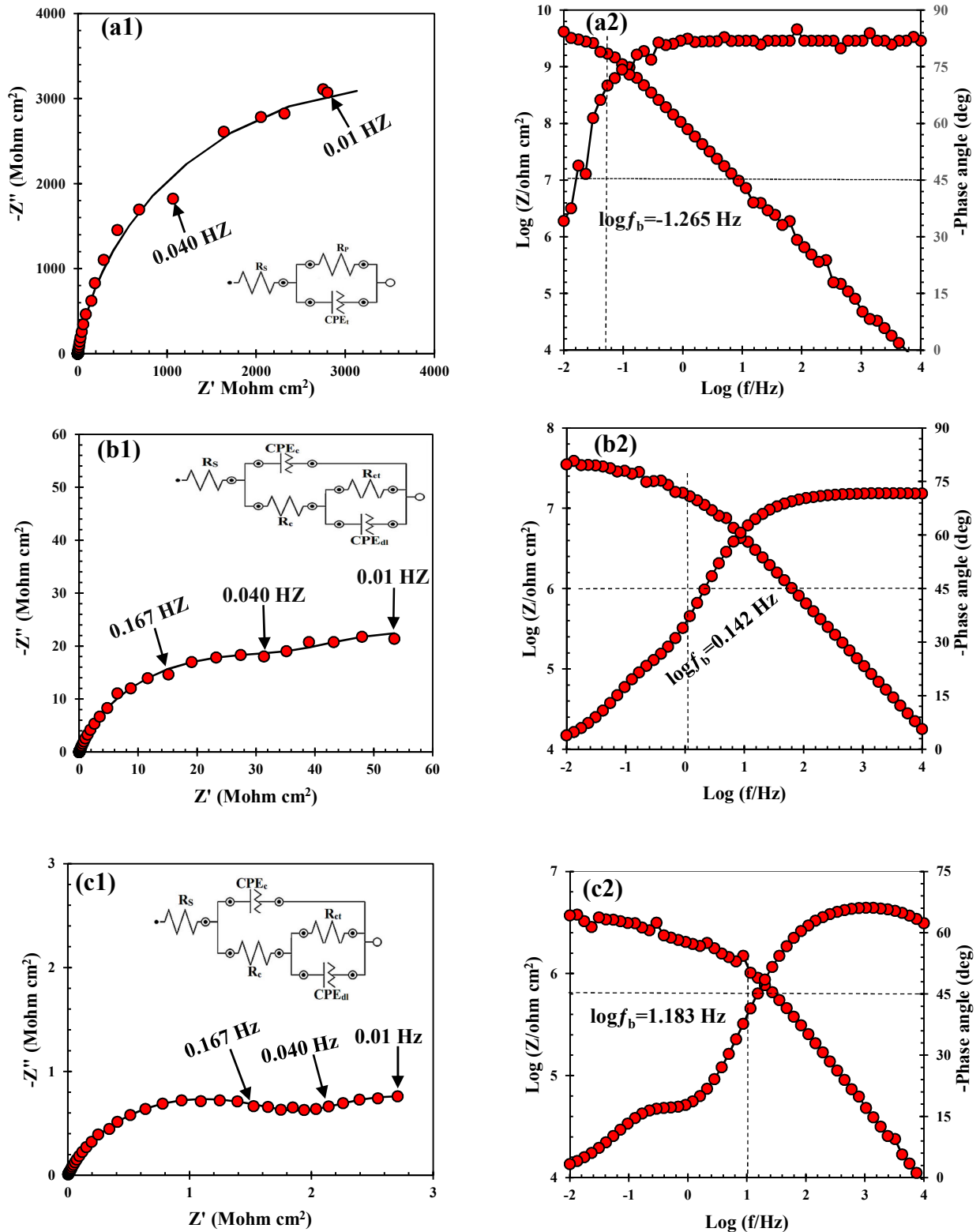


Figure 8: (a1, b1 and c1) Nyquist and (a2, b2 and c2) Bode plots of the epoxy coating applied on the VCC subjected to 3.5 wt% NaCl solution for (a1, a2) 3, (b1, b2) 15 and (c1, c2) 35 days immersion.

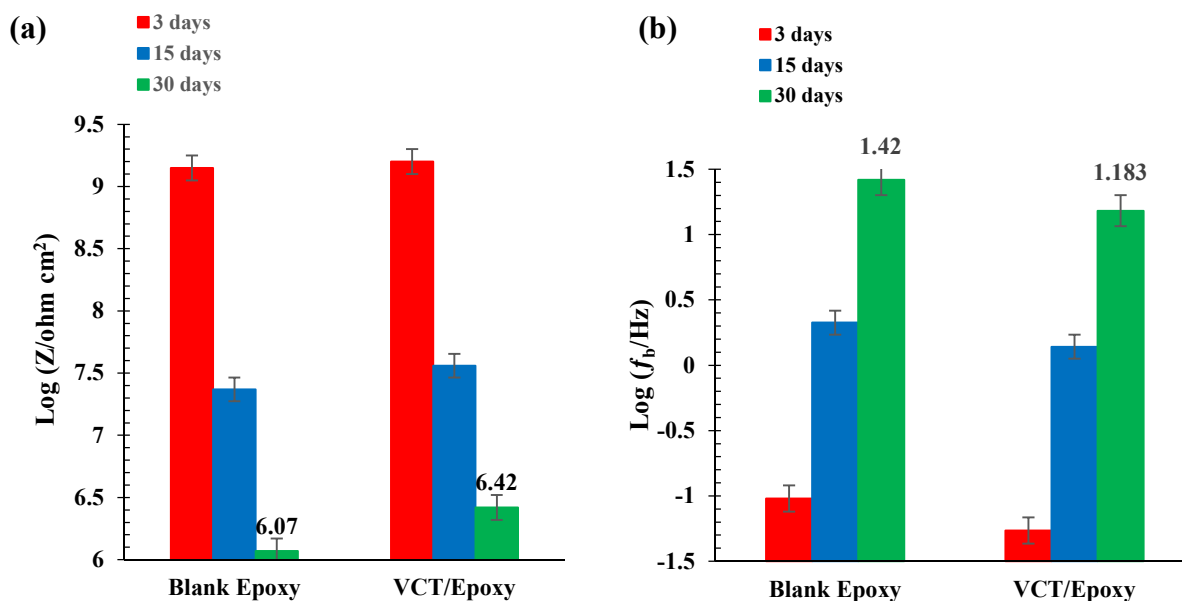


Figure 9: Impedance at 10 mHz (a) and breakpoint frequency (f_b) and (b) of the coatings applied on the steel specimens without and with VCC treatment subjected to 3.5 wt% NaCl solution for 3, 15 and 35 days immersion.

3.4. Cathodic delamination test

Most of the steel substrates coated with organic coatings are under cathodic protection. However these systems are influenced by a mechanical damage or defect in the coating inducing cathodic delamination or blisters. The holes and defects in the coating surface due to the easy access of cathodic reaction agents convert to cathodic areas. Applying a cathodic potential after the cathodic protection activates the cathodic reactions in the holes area and coating/metal interface. Hence, the effect of VCC treatment on the coating performance against cathodic delamination was studied. The study was carried out for 15 h on the samples with artificial defects (2 mm) under polarizing potential of 1.5 V at 23°C (compared with Ag/AgCl reference electrode). The results of the disbonded area after cathodic delamination are demonstrated in Figure 10. As it can be observed in Figure 10, the disbonded area decreases when the epoxy coating was applied with VCC treatment.

Although water and oxygen are available at disbonding front by penetrating through the coating/metal interface at the artificial defect areas, they could penetrate as a major source for the cathodic chemical reaction. The induction time is the time necessary for the corrosive electrolyte to attain the coating/metal interface by diffusion through the coating (Figure 10). Therefore, the increase of

induction time in the epoxy coating with VCC treatment may be relevant to reduce the access of corrosive electrolyte to interface metal/coating through blockage of the pores and channels epoxy coating.

These results reveal that recovery pull-off adhesion is a proper parameter for describe cathodic delamination behavior of the samples. Adhesion strength could be taken into account as a key parameter for desirable performance in cathodic disbondment [59]. The VCC treatment of steel surface enhances its roughness and recovery adhesion (According to previous results). VCC treatment raised the adhesion bonds between the epoxy coating and steel substrate through physical and chemical bonds (Section 3.2). The adhesion bonds between coating/substrate interfaces reduce the corrosion products.

The increase in cathodic protection time is responsible for the increase of hydroxyl ion creation rate which result in the increase of the pH scale at the coating/substrate interface. The hydroxyl ions can be created through oxygen reduction reaction (equation 7). As well as in this study a potential of -1.5 V (compared with Ag/AgCl reference electrode) is applied on the coatings with artificial defects. This reaction (equation 8) is responsible for the creation of hydroxyl ions.



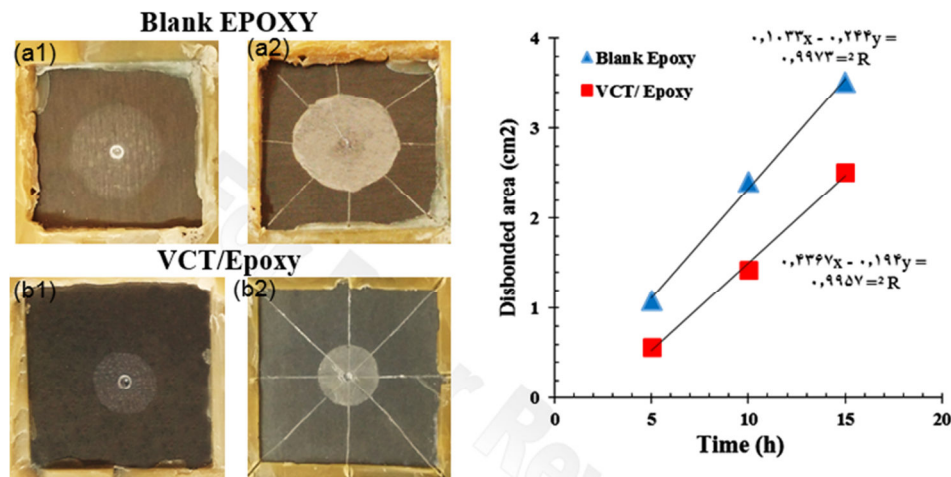


Figure 10: The rate of cathodic delamination of blank epoxy (a1, a2) and VCC/Epoxy (b1, b2) samples after different disbonding times.

The VCC treatment substrate can reduce the cathodic activity of metal substrate through covering the cathodic sites. Reduction of activity of metal substrate leads to a reduction in the production rate of hydroxyl ions (responsible for cathodic disbonding). Also, as stated by E-pH diagram of the vanadium component [60] it can be regarded that the vanadium oxide is stable at high alkaline state ($\text{pH} > 11$). Hence, the vanadium hydroxides convert to vanadium oxide, with increase of pH at the defect site. All these factors, especially, the decrease of cathodic activity and enhancing adhesion resistance affect in the increase of the epoxy coating resistance against cathodic delamination over the metal substrate.

3.5. EIS investigation of VCC/Epoxy and blank epoxy samples with artificial defect

In general, the EIS experiments presented can be divided into two groups: 1) Measurements on the intact coatings and 2) Measurements on defect coatings. The EIS is a suitable way to study the coating delamination and the corrosion products. The effect of VCC treatment of steel is studied on the corrosion protection attributes of the epoxy coating using EIS analysis. The test OCP on the coatings with an artificial defect (diameter = 2 mm) is presented in Table 5. Typical Bode and Nyquist diagrams of the coatings subjected to cathodic delamination test are depicted in Figure 11.

Bode plots demonstrate that only one time constant is observed for blank and VCC samples. This may indicate that the corrosion process on these samples is mostly under charge transfer process. The Nyquist diagrams show that VCC treatment of the mild steel increases the impedance. This study showed lower delamination VCC samples compared with the blank samples [61, 62]. Table 5 demonstrates variations of resistance and capacitance parameters extracted from impedance data by a simple equivalent circuit shown in Figure 11, where R_s , R_t and CPE_t are the solution resistance, total resistance ($R_t = \text{charge transfer resistance } (R_{ct}) + \text{coating resistance } (R_c)$) and total steady phase element, respectively. The coating delamination growth could be responsible for changes R and C values of the disbonded area [62–64]. In case of the samples modified by VCC, a considerable increase in the resistance, and diminution in capacitance indicates the delamination decrease. These results can be due to the enhancement of the adhesion properties and the decrease of electrochemical activity of the steel surface by VCC treatment. These observations show that interfacial bonding between the substrate and epoxy coating has a main role during the delamination process. Applying VCC before epoxy coating can provide strong interfacial bonding between the epoxy coating and the steel substrate.

Table 5: OCP values and the electrochemical parameters of Nyquist and Bode charts shown in Figures 11.

| Sample | R_t ($k\Omega\text{ cm}^2$) | CPE_t ($\mu F\text{ cm}^{-2}$) | | $OCP_{Ag/AgCl}$ (V) |
|-----------|---------------------------------|--|-----------------|---------------------|
| | | Y_0 ($\mu\Omega^{-1}\text{ cm}^{-2}\text{ S}^n$) | N | |
| Untreated | 18.1 ± 1.4 | 74 | 0.87 ± 0.02 | -0.39 ± 0.02 |
| VCT/Epoxy | 23.2 ± 1.8 | 48 | 0.88 ± 0.03 | -0.36 ± 0.04 |

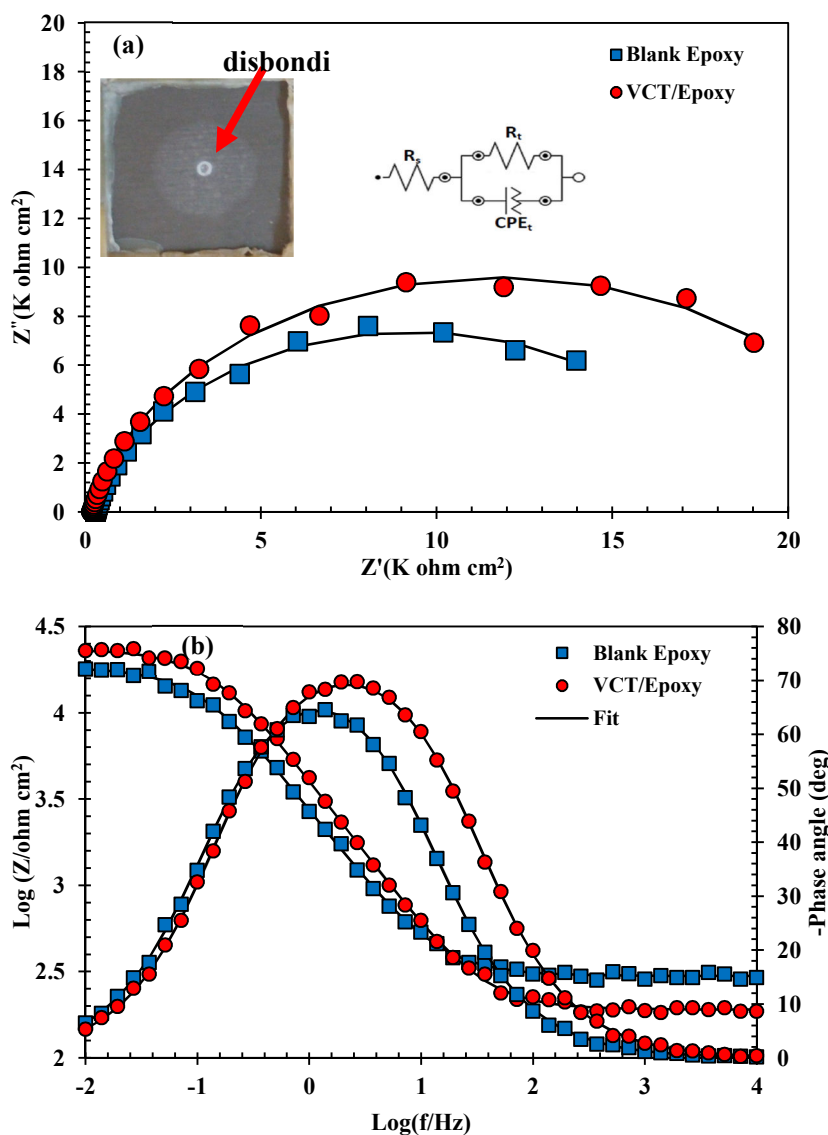


Figure 11: Nyquist (a) and Bode (b) diagrams of the blank epoxy and VCC/Epoxy samples with artificial defect.

4. Conclusion

In this study, the behavior of corrosion resistance, adhesion and cathodic delamination of epoxy coating with and without VCC was investigated via various analytical techniques. The main results obtained are:

1) The results obtained from FE-SEM analysis showed that the VCC is composed of closed-pack fine particles. Image J software also confirmed that the VCC layer is composed of nanoparticles with less than 30 nm particle size. Furthermore, the elemental mapping of EDX micrographs illustrated that the

coating mostly contains of vanadium and oxygen to form vanadium oxides/hydroxides. EDX shows the uniform distribution of V along the surface of VCC sample. 2) The results of surface topography were investigated by AFM. These results showed the increase of Rrms value from 18.65 to 66.48 nm for VCC treatment of steel. Hence, it may reduce the cathodic delamination of the thermoset coatings due to

the increase of interactions between the coatings and St-37 substrates. 3) EIS showed that VCC chemical treatments provide higher degree of corrosion protection for epoxy coating by limiting the cathodic and anodic reaction. VCC treatment reduced the cathodic delamination area in compare to the blank epoxy samples by increasing the adhesion strength and decreasing the cathodic activity.

5. References

1. Y. Hao, F. Liu, E. H. Han, S. Anjum, and G. Xu, The mechanism of inhibition by zinc phosphate in an epoxy coating, *Corr. Sci.*, 69(2013), 77-86.
2. J. Hou, G. Zhu, J. Xu, H. Liu, Anticorrosion performance of epoxy coatings containing small amount of inherently conducting PEDOT/PSS on hull steel in seawater, *J. Mater. Sci. Technol.*, 7(2013), 678-684.
3. X. Liu, J. Xiong, Y. Lv, Y. Zuo, Study on corrosion electrochemical behavior of several different coating systems by EIS, *Prog. Org. Coat.*, 64(2009), 497-503.
4. M. Gharagozlou, B. Ramezanzadeh, Z. Baradaran, Synthesize and characterization of a novel anticorrosive cobalt ferrite nanoparticles dispersed in silica matrix (CoFe₂O₄-SiO₂) to improve the corrosion protection performance of epoxy coating, *Appl. Surf. Sci.*, 377(2016), 86-98.
5. M. Ramezanzadeh, G. Bahlakeh, B. Ramezanzadeh, Development of a nanostructured Ce(III)-Pr(III) film for excellently corrosion resistance improvement of epoxy/polyamide coating on carbon steel, *J. Alloy Compoun.*, 792(2019), 375-388.
6. B. Ramezanzadeh, M. Attar, Studying the effects of micro and nano sized ZnO particles on the corrosion resistance and deterioration behavior of an epoxy-polyamide coating on hot-dip galvanized steel, *Prog. Org. Coat.*, 71.3(2011), 314-328.
7. T. Wu, A. Foyet, A. Kodentsov, L. van der Ven, R. van Benthem, G. de With, Wet adhesion of epoxy-amine coatings on 2024-T3 aluminum alloy, *Mater. Chem. Phys.*, 145(2014), 342-349.
8. G. Bahlakeh, B. Ramezanzadeh, M. Ramezanzadeh, Cerium oxide nanoparticles influences on the binding and corrosion protection characteristics of a melamine-cured polyester resin on mild steel: An experimental, density functional theory and molecular dynamics simulation study, *Corr. Sci.*, 118(2017), 69-83.
9. M. Ghaffari, M. R. Saeb, B. Ramezanzadeh, P. Taheri, Demonstration of epoxy/carbon steel interfacial delamination behavior: Electrochemical impedance and X-ray spectroscopic analyses, *Corro. Sci.*, 102(2016), 326-337.
10. N. Rezaee, M. Attar, B. Ramezanzadeh, Studying corrosion performance, microstructure and adhesion properties of a room temperature zinc phosphate conversion coating containing Mn²⁺ on mild steel, *Surf. Coat. Technol.*, 236(2013), 361-367.
11. J. Marsh, J. Scantlebury, S. Lyon, The effect of surface/primer treatments on the performance of alkyd coated steel, *Corros. Sci.*, 43(2001), 829-852.
12. S. Adhikari, K. A. Unocic, Y. Zhai, G. Frankel, J. Zimmerman, W. Fristad, Hexafluorozirconic acid based surface pretreatments: Characterization and performance assessment, *Electrochim. Acta.*, 56(2011), 1912-1924.
13. G. Gusmano, G. Montesperelli, M. Rapone, G. Padeletti, A. Cusmà, S. Kaciulis, Zirconia primers for corrosion resistant coatings, *Surf. Coat. Technol.*, 201(2007), 5822-5828.
14. R. D. Maggio, L. Fedrizzi, S. Rossi, Effect of the chemical modification of the precursor of ZrO₂ films on the adhesion of organic coatings, *J. Adh. Sci. Technol.*, 15(2001), 793-808.
15. M. Tabatabaei Majd, T. Shahrabi, B. Ramezanzadeh, The role of neodymium based thin film on the epoxy/steel interfacial adhesion and corrosion protection promotion, *Appl. Surf. Sci.*, 464(2019), 516-533.
16. T. S. Narayanan, Surface pretreatment by phosphate conversion coatings—a review, *Rev. Adv. Mater. Sci.*, 9(2005), 130-177.
17. M. Fedel, M. E. Druart, M. Olivier, M. Poelman, F. Deflorian, S. Rossi, Compatibility between cathodic electro-coating and silane surface layer for the corrosion protection of galvanized steel, *Prog. Org. Coat.*, 69(2010), 118-125.
18. J. Gailen, E. Vaughan, Protective coatings for metals, Charles Griffin & Co, Ltd., (1979), 97.
19. T. Hanawa, M. Ota, Characterization of surface film formed on titanium in electrolyte using XPS, *Appl. Surf. Sci.*, 55(1992), 269-276.
20. H. E. Mohammadloo, A. Sarabi, R. M. Hosseini, M. Sarayloo, H. Sameie, R. Salimi, A comprehensive study of the green hexafluorozirconic acid-based conversion coating, *Prog. Org. Coat.*, 77(2014), 322-330.

21. N. Jantaping, C.A. Schuh, Y. Boonyongmaneerat, Influences of crystallographic texture and nanostructural features on corrosion properties of electrogalvanized and chromate conversion coatings, *Surf. Coat. Technol.*, 329(2017), 120-130.
22. A. S. Hamdy, I. Doench, H. Möhwald, Smart self-healing anti-corrosion vanadia coating for magnesium alloys, *Prog. Org. Coat.*, 72(2011), 387-393.
23. X. Zhang, W. Sloof, A. Hovestad, E. Van Westing, H. Terryn, J. De Wit, Characterization of chromate conversion coatings on zinc using XPS and SKPFM, *Surf. Coat. Technol.*, 197(2005), 168-176.
24. X. Zhang, C. Van den Bos, W. Sloof, A. Hovestad, H. Terryn, J. De Wit, Comparison of the morphology and corrosion performance of Cr (VI)-and Cr (III)-based conversion coatings on zinc, *Surf. Coat. Technol.*, 199(2005), 92-104.
25. R. Twite, G. Bierwagen, Review of alternatives to chromate for corrosion protection of aluminum aerospace alloys, *Prog. Org. Coat.*, 33(1998), 91-100.
26. S. Cohen, Review: Replacements for chromium pretreatments on aluminum, *Corrosion*, 51(1995), 71-78.
27. A. Pereira, G. Pimenta, B. Dunn, Assessment of chemical conversion coatings for the protection of aluminium alloys, *ESA Sci. Technical Memor.*, 276(2008), 77-83.
28. C. Tomachuk, C. Elsner, A. Di Sarli, O. Ferraz, Corrosion resistance of Cr (III) conversion treatments applied on electrogalvanized steel and subjected to chloride containing media, *Mater. Chem. Phys.*, 119(2010), 19-29.
29. B. Ramezanzadeh and M. Attar, Effects of Co(II) and Ni (II) on the surface morphology and anticorrosion performance of the steel samples pretreated by Cr (III) conversion coating, *J. Sci. Eng.*, 68(2012), 015008-1.
30. T. Bellezze, G. Roventi, R. Fratesi, Electrochemical study on the corrosion resistance of Cr III-based conversion layers on zinc coatings, *Surf. Coat. Technol.*, 155(2002), 221-230.
31. K. Cho, V. S. Rao, H. Kwon, Microstructure and electrochemical characterization of trivalent chromium based conversion coating on zinc, *Electrochim. Acta.*, 52(2007), 4449-4456.
32. A. Magalhaes, I. Margarit, O. Mattos, Molybdate conversion coatings on zinc surfaces, *J. Electroanaly. Chem.*, 572(2004), 433-440.
33. T. Xu, C. Xie, Tetrapod-like nano-particle ZnO/acrylic resin composite and its multi-function property, *Prog. Org. Coat.*, 46(2003), 297-301.
34. C. Da Silva, I. Margarit-Mattos, O. Mattos, H. Perrot, B. Tribollet, V. Vivier, The molybdate-zinc conversion process, *Corros. Sci.*, 51(2009), 151-158.
35. H. Hassannejad, M. Moghaddasi, E. Saebnoori, A.R. Baboukani, Microstructure, deposition mechanism and corrosion behavior of nanostructured cerium oxide conversion coating modified with chitosan on AA2024 aluminum alloy, *J. Alloy Compoun.*, 725(2017), 968-975.
36. J. Sun, G. Wang, Preparation and corrosion resistance of cerium conversion coatings on AZ91D magnesium alloy by a cathodic electrochemical treatment, *Surf. Coat. Technol.*, 254(2014), 42-48.
37. Z. Mahidashti, B. Ramezanzadeh, G. Bahlakeh, Screening the effect of chemical treatment of steel substrate by a composite cerium-lanthanum nanofilm on the adhesion and corrosion protection properties of a polyamide-cured epoxy coating; Experimental and molecular dynamic simulations, *Prog. Org. Coat.*, 114(2018), 188-200.
38. H.R. Asemani, P. Ahmadi, A.A. Sarabi, H. Eivaz Mohammadloo, Effect of zirconium conversion coating: Adhesion and anti-corrosion properties of epoxy organic coating containing zinc aluminum polyphosphate (ZAPP) pigment on carbon mild steel, *Prog. Org. Coat.*, 94(2016), 18-27.
39. H. Eivaz Mohammadloo, A.A. Sarabi, Titanium composite conversion coating formation on CRS In the presence of Mo and Ni ions: Electrochemical and microstructure characterizations, *Appl. Surf. Sci.*, 387(2016), 252-259.
40. H. Eivaz Mohammadloo, A.A. Sarabi, Ti-Based conversion coatings on cold-rolled steel substrate: the effect of practical parameters and Ti source on surface and electrochemical properties, *Corrosion*, 72(2016), 791-804.
41. G. Kong, L. Lingyan, J. Lu, C. Che, Z. Zhong, Corrosion behavior of lanthanum-based conversion coating modified with citric acid on hot dip galvanized steel in aerated 1M NaCl solution, *Corros. Sci.*, 53(2011), 1621-1626.
42. X. Jiang, R. Guo, S. Jiang, Microstructure and corrosion resistance of Ce-V conversion coating on AZ31 magnesium alloy, *Appl. Surf. Sci.*, 341(2015), 166-174.
43. A. S. Hamdy, I. Doench, H. Möhwald, Intelligent self-healing corrosion resistant vanadia coating for AA2024, *Thin Solid Films*, 520(2011), 1668-1678.
44. Z. Zou, N. Li, D. Li, Corrosion protection properties of vanadium films formed on zinc surfaces, *Rare Metals.*, 30(2011), 146.
45. K. Li, J. Liu, T. Lei, T. Xiao, Optimization of process factors for self-healing vanadium-based conversion coating on AZ31 magnesium alloy, *Appl. Surf. Sci.*, 353(2015), 811-819.
46. A. S. Hamdy, D. Butt, Novel anti-corrosion nano-sized vanadia-based thin films prepared by sol-gel method for aluminum alloys, *J. Mater. Proces. Technol.*, 181(2007), 76-80.
47. H. Guan, R. Buchheit, Corrosion protection of aluminum alloy 2024-T3 by vanadate conversion coatings, *Corrosion.*, 60(2004), 284-296.
48. K. Yang, M. Ger, W. Hwu, Y. Sung, Y. C. Liu, Study of vanadium-based chemical conversion coating on the corrosion resistance of magnesium alloy, *Mater. Chem. Phys.*, 101(2007), 480-485.
49. A. S. Hamdy, A. M. Beccaria, Corrosion protection performance of thickened oxide conversion coatings

- containing vanadium ions formed on aluminum composites, *Corros. Preven. Control.*, 48(2001), 143-149.
50. A. S. Hamdy, I. Doench, H. Möhwald, Vanadia-based coatings of self-repairing functionality for advanced magnesium Elektron ZE41 Mg–Zn–rare earth alloy, *Surf. Coat. Technol.*, 206(2012), 3686-3692.
 51. A. S. Hamdy, I. Doench, H. Möhwald, Assessment of a one-step intelligent self-healing vanadia protective coatings for magnesium alloys in corrosive media, *Electrochim. Acta.*, 56(2011), 2493-2502.
 52. M. Motamedi, M. Attar, Nanostructured vanadium-based conversion treatment of mild steel substrate: formation process via noise measurement, surface analysis and anti-corrosion behavior, *RSC Adv.*, 6(2016), 44732-44741.
 53. C. A. Schneider, W. S. Rasband, K. W. Eliceiri, NIH Image to ImageJ: 25 years of image analysis, *Nature Method.*, 9(2012), 671.
 54. Z. Zou, N. Li, D. Li, H. Liu, S. Mu, A vanadium-based conversion coating as chromate replacement for electrogalvanized steel substrates, *J. Alloy Compoun.*, 509(2011), 503-507.
 55. M. Raposo, Q. Ferreira, P. Ribeiro, A guide for atomic force microscopy analysis of soft-condensed matter, *Modern Res. Educ. Topic Micros.*, 1(2007), 758-769.
 56. R. J. Good, Contact angle, Wetting, and adhesion: a critical review, *J. Adh. Sci. Technol.*, 6(1992), 1269-1302.
 57. B. Ramezanzadeh, M. Attar, Studying the corrosion resistance and hydrolytic degradation of an epoxy coating containing ZnO nanoparticles, *Mater. Chem. Phys.*, 130(2011), 1208-1219.
 58. B. Ramezanzadeh, M. Rostami, The effect of cerium-based conversion treatment on the cathodic delamination and corrosion protection performance of carbon steel-fusion-bonded epoxy coating systems, *Appl. Surf. Sci.*, 392(2017), 1004-1016.
 59. P. A. Sørensen, K. Dam Johansen, C. Weinell, S. Kiil, Cathodic delamination: Quantification of ionic transport rates along coating–steel interfaces, *Prog. Org. Coat.*, 68(2010), 70-78.
 60. K. Post, R. Robins, Thermodynamic diagrams for the vanadium-water system at 298·15K, *Electrochim. Acta.*, 21(1976), 401-405.
 61. J. B. Jorcin, E. Aragon, C. Merlatti, N. Pèbère, Delaminated areas beblankh organic coating: A local electrochemical impedance approach, *Corros. Sci.*, 48(2006), 1779-1790.
 62. R. Naderi, M. Attar, The role of zinc aluminum phosphate anticorrosive pigment in protective performance and cathodic disbondment of epoxy coating, *Corros. Sci.*, 52(2010), 1291-1296.
 63. R. Hirayama, S. Haruyama, Electrochemical impedance for degraded coated steel having pores, *Corrosion.*, 47(1991), 952-958.
 64. F. Mansfeld, C. Tsai, Determination of coating deterioration with EIS: I. Basic relationships, *Corrosion.*, 47(1991), 958-963.

How to cite this article:

M. S. Dehghan, M. M. Attar, Enhancement of Adhesion Properties, Corrosion Resistance and Cathodic Disbonding of Mild Steel-Epoxy Coating Systems By Vanadium Conversion Coating, *Prog. Color Colorants Coat.*, 13 (2020), 223-238.

